Fluorescent Taxoids as Probes of the Microtubule Cytoskeleton

Juan A. Evangelio,[1] Miguel Abal,[1] Isabel Barasoain,[1] André A. Souto,[2] M. Pilar Lillo,[3] A. Ulises Acuña,[3] Francisco Amat-Guerri,[2] and José M. Andreu[1]*

[1]*Centro de Investigaciones Biológicas, CSIC, Madrid, Spain*
[2]*Instituto de Química Orgánica, CSIC, Madrid, Spain*
[3]*Instituto de Química-Física Rocasolano, CSIC, Madrid, Spain*

Microtubules are specifically and efficiently visualized with the new fluorescent taxoids 7-O-[N-(4 -fluoresceincarbonyl)-L-alanyl]taxol (FLUTAX) and 7-O-[N-(4 -tetramethyl-rhodaminecarbonyl)-L-alanyl]taxol (ROTAX). Similarly to taxol, FLUTAX and ROTAX are able to drive inactive GDP-liganded tubulin into microtubule assembly. One molecule of FLUTAX binds per $\alpha\beta$-tubulin dimer assembled, competing with taxol for the same microtubule binding site with an eightfold smaller relative affinity. FLUTAX-induced microtubule elongation is markedly Mg^{2+}-dependent, encompassing the binding of one Mg^{2+} ion more per tubulin dimer polymerized than in the case of taxol. A small perturbation of the absorption spectrum of bound FLUTAX is consistent with a cationic microenvironment relative to the solution. The fluorescence anisotropy of FLUTAX increases by an order of magnitude upon binding to microtubules and time-resolved measurements indicate that the fluorescein moiety remains considerably mobile on a protein surface. The rate of labeling suggests that this is the outer microtubule wall. Alternatively, the microtubule lumen would be functional. FLUTAX- and ROTAX-induced microtubules, radial structures, and organized microtubule bundles are readily observed under the fluorescence microscope. Rapid and accurate visualization of native (or very mildly fixed) cytoplasmic and spindle microtubules of a variety of permeabilized cells is simply obtained with micromolar FLUTAX, with an advantage over immunofluorescence. In addition, FLUTAX labels the centrosomes of PtK2 cells more intensely than antibodies to α- or β-tubulin, and co-localizing with antibodies to γ-tubulin. Two brightly fluorescent spots, probably separating or duplicating centrioles, can be resolved in the centrosomes of interphase cells. This finding indicates that centrosomes may well be additional targets of action of taxoids. FLUTAX strongly labels microtubules near the spindle poles, as well as microtubules at the telophase spindle equator and the central part of the midbody in cytokinesis (instead of the dark zone frequently observed with immunofluorescence), suggesting a predominant interaction of FLUTAX with sites at which tubulin is newly polymerized. Nanomolar concentrations of FLUTAX also permit specific imaging of centrosomes, half-spindles and midbodies in growing U937 cells. Cell Motil. Cytoskeleton 39:73–90, 1998. 1998 Wiley-Liss, Inc.

INTRODUCTION

Microtubules are essential for the organization, cytoplasmic transport, motility, and division of eukaryotic cells. In addition, they are targets of antimitotic drugs, including colchicine, vinblastine, and taxol [Wilson and Jordan, 1994]. Tubulin was discovered as a colchicine binding protein that assembled to form microtubules [Taylor, 1965; Wilson and Friedkin, 1966; Weisenberg et al., 1968; Weisenberg, 1972; Lee and Timasheff, 1975]. However, the use of colchicine derivatives to visualize microtubules has been very limited [Clark and Garland, 1978; Moll et al., 1982], since the tubulin–colchicine complex inhibits the assembly and dynamics of microtubules by binding to their ends [Panda et al., 1995]. On the contrary, taxol, an antitumor drug, is an inducer of microtubule assembly [Schiff et al., 1979, 1980] and a stabilizing inhibitor of microtubule dynamics that binds to the microtubule wall [Parness and Horwitz, 1981; Horwitz, 1992; Derry et al., 1995]. Taxol is considered to bind to cellular microtubules [Manfredi et al., 1982], although it may have additional targets [Wolfson et al., 1997] (C. De Inés and I. Barasoain, unpublished observations). Until now, taxol binding has not been efficiently visualized.

Taxol induces microtubule formation by binding preferentially to assembled, rather than to unassembled, tubulin [Parness and Horwitz, 1981; Carlier and Pantaloni, 1983]. The binding of exactly one molecule of taxol per αβ-tubulin dimer polymerized completely bypasses the requirement of the γ phosphate of bound GTP for tubulin assembly [Díaz and Andreu, 1993]. Specific photoaffinity labeling with azidotaxol derivatives has mapped taxol-binding sequences at the N-terminal 31 residues and at positions 217–231 of the β-subunit [Rao et al., 1994, 1995]. The low-resolution structures of microtubules in solution show that taxol-induced microtubules have, on average, one protofilament less than is found in microtubules assembled with glycerol, microtubule-associated proteins, or docetaxel [Andreu et al., 1992, 1994]. Taxol binding also induces a 3.5% lengthening of the 4-nm axial spacing between tubulin monomers along protofilaments [Vale et al., 1994; Arnal and Wade, 1995] and modifies the flexibility of microtubules [Dye et al., 1993; Venier et al., 1994; Mickey et al., 1995]. From structural [Andreu et al., 1992], thermodynamic [Díaz et al., 1993] and kinetic studies of the intermediates of taxoid-induced microtubule assembly [Díaz et al., 1996], we have proposed that taxol binding: (1) modifies the lateral interactions between tubulin molecules in microtubules, possibly by binding between protofilaments; (2) switches GDP-tubulin from the inactive to the assembling conformation; and (3) probably induces the lateral accretion of tubulin oligomers, transforming them into active microtubule nucleating species. The mid-resolution structure of tubulin in zinc-induced sheets has shown a single taxol binding site per dimer, located approximately between the protofilaments [Nogales et al., 1995; Wolff et al., 1996]; however, the antiparallel orientation of these protofilaments relative to microtubules precludes deducing from these data the position of taxol in microtubules.

It can be expected that, in analogy to fluorescent derivatives of phalloidin [Wulf et al., 1979] widely employed to study actin microfilaments, fluorescent taxol derivatives could be extremely useful to study cellular microtubules, as well as the mechanisms of microtubule assembly and stabilization by taxol. The complex chemistry of taxol [Kingston, 1994; Nicolaou and Guy, 1995] made difficult obtaining water-soluble significantly active derivatives labeled with appropriate fluorescent groups, but this was recently accomplished [Souto et al., 1995]. In the present work we have used fluorescent taxoids with adequate affinity and selectivity to probe the taxol binding site of in vitro assembled and cellular microtubules. Cytoplasmic microtubules, mitotic spindles and centrosomes are directly and specifically visualized and studied with fluorescent taxoids.

MATERIALS AND METHODS
Fluorescent Taxoids and Other Materials

7-O-[N-(4´-fluoresceincarbonyl)-L-alanyl]taxol (FLUTAX) and 7-O-[N-(4-coumarincarbonyl)-L-alanyl]-taxol (CUTAX) were obtained by the reaction of 7-O-(L-alanyl)taxol with the corresponding amine-reactive fluorescent dye, as described [Souto et al., 1995]. Other fluorescent taxoids were obtained by this general method and purified by preparative Thin layer chromatography (TLC). They gave a single spot on TLC plates with several eluents. 2´-O-Acetyl-7-O-[N-(4´-fluoresceincarbonyl)-L-alanyl]taxol (2´-Ac-FLUTAX) was obtained from 2´-O-acetyltaxol [Mellado et al., 1984] by its conversion into 2´-O-acetyl-7-O-(L-alanyl)taxol and subsequent reaction with 4´-carboxyfluorescein succinimidyl ester (Molecular Probes C-2210, Eugene, OR). N-(4´-fluoresceincarbonyl)-L-alanine methyl ester was prepared by the reaction of the same succinimidyl ester with L-alanine methyl ester hydrochloride (Fluka 05200, Buchs, Switzerland).

7-O-[N-(4´-tetramethylrhodaminecarbonyl)-L-alanyl]-taxol (ROTAX) was synthesized from 7-O-(L-alanyl)-taxol and 4´-carboxytetramethylrhodamine succinimidyl ester (Molecular Probes C-2211), and its structure (Fig. 1) was confirmed as follows. HRFAB+-MS (m-NBA), m/z: 1337.5141 (MH+, calculated for $C_{83}H_{85}N_4O_{19}$ 1337.5182). ^{1}H NMR (300 MHz, CDCl$_3$, 298 K, TMS): δ = 8.38 (s, 1H, H-3 R), 8.20 (d, 1H, H-5 R), 8.07 (d, 2H, o-H of Ph(a)), 7.69 (d, 2H, o-H of Ph(c)), 7.69-7.19 band, 11H,
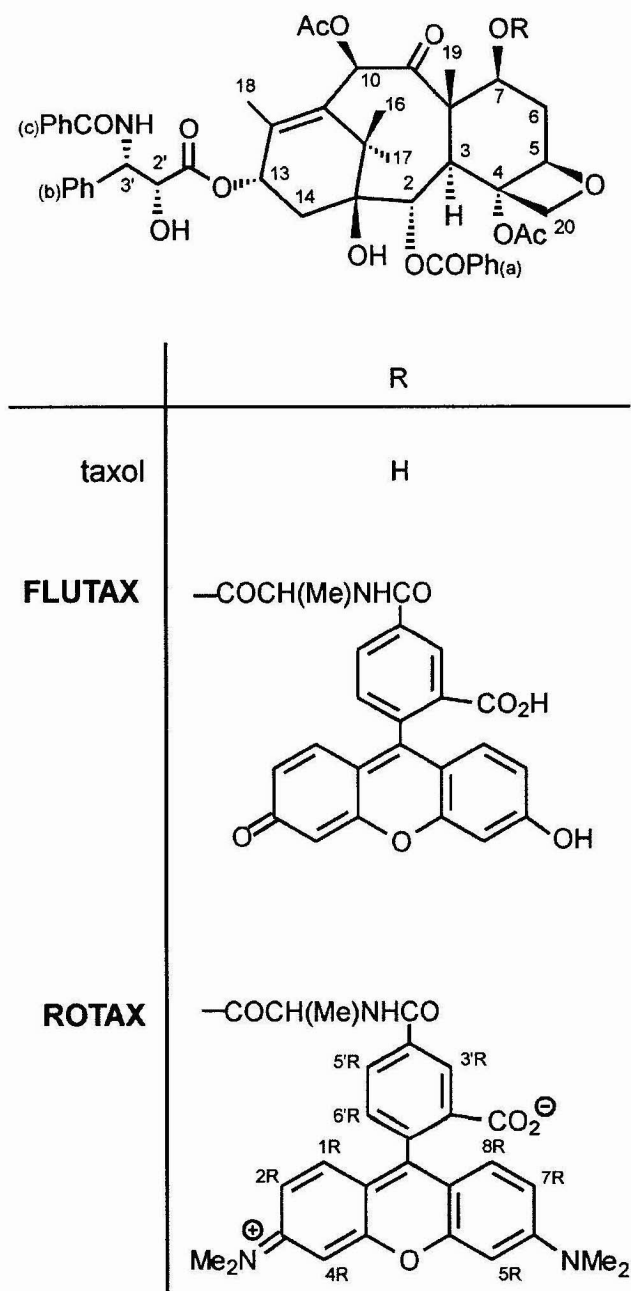
Fig. 1. Chemical structures of the fluorescent taxol derivatives employed in this work.

(s, 3H, 10-CH$_3$CO), 2.09 (m, 1H, H-6b), 1.79 (s, 6H, H-18, H-19), 1.34 (d, 3H, CH$_3$ of Ala), 1.18 (s, 3H, H-17), 1.16 (s, 3H, H-16).

FLUTAX, CUTAX, ROTAX, and 2'-Ac-FLUTAX had ultraviolet (UV)-visible absorbance and fluorescence emission spectra in accordance with the respective chromophores. High-performance liquid chromatography (HPLC) purity (228 nm) was: FLUTAX 91% (0.3% taxol), 2'-Ac-FLUTAX 89% (undetectable taxol, 0.8% FLUTAX) (C-18 25 × 0.4-cm column, 20–80% acetonitrile gradient in 0.05% trifluoroacetic acid in water), ROTAX 95% (undetectable taxol) (C-4 column in the same eluent). The concentrations of FLUTAX, ROTAX, and 2'-Ac-FLUTAX were determined spectrophotometrically in 0.5% sodium dodecyl sulfate (SDS), 50 mM sodium phosphate buffer, pH 7.0, respectively, employing the practical extinction coefficients $\epsilon_{458\ nm} = 23{,}100 \pm 600\ M^{-1}\ cm^{-1}$, $\epsilon_{555\ nm} \approx 80{,}000\ M^{-1}\ cm^{-1}$, $\epsilon_{458\ nm} = 16{,}600 \pm 600\ M^{-1}\ cm^{-1}$, obtained by weighing and by SDS solubilization of the taxoids. Similar to taxol [Song et al., 1996], FLUTAX partially adsorbs to glass and plastic containers, from which it can be recovered with 0.5% SDS. Without SDS, about 15–25% of 2- to 25-µM FLUTAX solutions would adsorb to the walls of a spectrophotometer cell. Ligand solubilities were determined by ultracentrifugation of 0.2-ml aliquots at 100,000g and 25°C during 10 min, and measuring the concentration in the upper and lower half of the tubes.

Taxol (Paclitaxel) was in part a gift from Bristol-Myers-Squibb, Princeton, N.J., the owner of the registered trademark. Docetaxel (Taxotere) was a gift from Rhone-Poulenc Rorer, Autong, France. SDS was from BioRad, Hercules, CA. Other chemicals were as described [Díaz and Andreu, 1993; De Inés et al., 1994], unless otherwise indicated.

Proteins, Microtubule Assembly, Binding of Ligands, and Spectroscopic Measurements

Purified guanosine diphosphate (GDP)-tubulin was prepared from calf brain as described elsewhere [Díaz and Andreu, 1993]. GDP from Sigma (St. Louis, MO), sodium salt type I (undetectable GTP in HPLC) was now employed, giving 95 ± 3% GDP-liganded tubulin in the HPLC nucleotide analysis. GDP-tubulin was assembled with a 1.2:1 taxoid–tubulin molar ratio (except otherwise indicated) in PEGM buffer, pH 6.6 at 37°C for 2 hr, followed by 10-min centrifugation of 0.2-ml aliquots at 100,000g, 37°C. Pellets were resuspended in cold PEDTA buffer or in 10 mM sodium phosphate buffer–0.25% SDS, pH 7.0. FLUTAX and tubulin concentrations in pellets and supernatants were determined fluorometrically in aliquots diluted in 0.25% SDS with the appropriate standards, and taxol was determined by HPLC with docetaxel as an internal standard. Bovine microtubule

m- and p-H of Ph(a), o-, m-, and p-H of Ph(b), m- and p-H of Ph(c)), 7.00 (d, 1H, NH) 6.51-6.48 (band, 2H, H-2R, H-7R), 6.43 and 6.42 (two s, 2H, H-4R, H-5R), 6.37-6.28 (band, 3H, H-1R, H-7R, H-6 R), 6.27 (s, 1H, H-10), 6.12 (t, 1H, H-13), 5.75-5.63 (band, 3H, H-2, H-7, H-3'), 4.90 (m, 2H, H-5, CH of Ala), 4.74 (d, 1H, H-2'), 4.25 (d, 1H, H-20a), 4.16 (d, 1H, H-20b), 3.88 (d, 1H, H-3), 3.57 (broad s, 2'-OH), 2.92 (s, 12H, 2xN(CH$_3$)$_2$), 2.52 (m, 1H, H-6a), 2.34 (s, 3H, 4-CH$_3$CO), 2.30 (m, 2H, H-14), 2.24

protein was prepared as described [de Pereda et al., 1995] and assembled (4 mg/ml) in 100 mM Pipes, 1 mM EGTA, 1 mM $MgCl_2$, 1 mM GTP, pH 6.9, at 37°C. Aliquots of noncentrifuged microtubules were examined by fluorescence microscopy (see below) or adsorbed to Formvar and carbon-coated copper grids, negatively stained with 2% uranyl acetate and photographed with a Philips EM400 electron microscope.

Absorption spectra were recorded with Varian Cary 3E and Hitachi U2000 spectrophotometers. Light scattering by microtubules was corrected by double logarithmic back-extrapolation from non absorbing spectral regions [Andreu and Timasheff, 1984]. Fluorescence spectra were acquired with Shimadzu RF540 and SLM 8000 D spectrofluorimeters. Fluorescence lifetime, steady-state, and time-resolved anisotropy measurements were performed as described elsewhere [Mateo et al., 1991].

Cell Lines, Cytoskeletons, and Fluorescence Microscopy

PtK2 potoroo epithelial-like kidney cells, U937 monocytic human leukemia and K562 human myelocytic leukemia cells were grown as described previously (De Inés et al., 1994). Neuro 2A mouse neuroblastoma was grown in DME nutrient mixture F-12 Ham (Sigma), with 10% fetal calf serum (FCS), 2 mM glutamine, nonessential amino acids, and antibiotics. Trypanosoma cruzi strain Tulahuén [Tagliaferro and Pizzi, 1955] was cultured as described [Baum et al., 1981]. Coverslip-attached PtK2 cytoskeletons were prepared as described [De Inés et al., 1994]. They were either directly observed or fixed with 0.2% glutaraldehyde in PEM at room temperature for 15 min, and then for 15 min in 2 mg/ml $NaBH_4$. These mildly fixed cytoskeletons were sequentially incubated with DM1A monoclonal antibody (Sigma; diluted 1:400 in PBS–10 mg/ml BSA, 1 hr at 37°C), biotinylated sheep antimouse immunoglobulins (Amersham; diluted 1:400, 45 min), and streptavidin–Texas Red (Amersham; Amersham, Buckinghamshire, U.K.); diluted 1:400, 30 min). 1 µM FLUTAX was added into the three incubations. In other experiments, unfixed PtK2 cytoskeletons labeled with FLUTAX were photographed prior to fixation with methanol (10 min at −20°C) and acetone (6 min at −20°C), incubated with TU-30 mouse monoclonal antibody to γ-tubulin, diluted 1:8 [Nováková et al., 1996] and C85 purified rabbit monospecific antibodies to α-tubulin [Arévalo et al., 1990], 40 µg/ml for 1 hr at 37°C, followed by incubation with biotinylated sheep antimouse immunoglobulins (1:1,000) for 45 min, and finally with streptavidin-Texas red (1:1,000) and fluoresceinated goat antirabbit immunoglobulins (Sigma, 1:40) for 30 min. Cells and cytoskeletons were mounted in 0.13 M glycine buffer pH 8.6 containing 0.20 M NaCl, 70% glycerol, and 0.05 µg/ml Hoescht 33342 (Sigma). Living

cells were mounted in fluorescent taxoid containing culture medium, to which propidium iodide (1 µg/ml) (Sigma) and Hoescht 33342 (0.05 µg/ml) had been added just before observation (living cells excluded propidium iodide and their nuclei were stained with Hoescht 33342). Cells and cytoskeletons were observed through 63× Plan-Apochromat and Plan-Neofluar objectives with Zeiss Axioplan epifluorescence microscopes with appropriate filter combinations for Hoescht 33342, fluorescein, rhodamine, and Texas red; their images were recorded separately, either on Kodak TMAX film and scanned with an Ektron 1412 digital imaging camera system, or with a Photometrics 200 KAF-1400 cooled CCD camera and IPLab Spectrum software, and were printed with Adobe Photoshop .

RESULTS

The chemical structures of fluorescein and rhodamine labeled taxoids prepared by conjugation through the free amino group of 7-O-(L-alanyl)taxol with amine-reactive dyes [Souto et al., 1995] (Materials and Methods) are shown in Figure 1. FLUTAX, the main probe employed in this work, is fully (>0.2 mM) soluble in 10 mM sodium phosphate buffer at pH 8.5 and insoluble at pH 4.0. The solubility of FLUTAX and 2 -Ac-FLUTAX at pH 7.0 is approximately 80% of the initial concentration (<0.1 mM), 50% at pH 6.6, and further reduced by 7 mM $MgCl_2$. The solubility of FLUTAX increases in the presence of tubulin and has been employed without problems in cell culture media containing 10% FCS. The solubility of ROTAX in aqueous buffers at neutral pH is approximately 1 µM.

Microtubule Assembling and Binding Activities of Fluorescent Taxoids

A stringent biochemical test for the activity of taxoids is their ability to induce the assembly of microtubules from the otherwise inactive GDP-liganded form of tubulin [Díaz and Andreu, 1993]. Figure 2A shows the time courses of assembly of microtubules induced by taxol (line 1), FLUTAX (line 2), and the rhodamine analogue ROTAX (line 3), indicating that the fluorescent analogues are slightly slower assembly inducers than taxol. As negative controls we employed the fluorescein moiety, N-(4 -fluoresceincarbonyl)-L-alanine methyl ester (line 4), and 2 -Ac-FLUTAX (line 5), which lacks the essential 2 hydroxy group of the taxol side chain [Williams et al., 1996; Jimenez-Barbero et al., submitted]. The polymers induced by FLUTAX and ROTAX are microtubules, as shown in Figure 2B,C, although possible modifications in their substructure, as those induced by the parent drug (see Introduction), are still to be addressed. Sedimentation measurements of assembled tubu-
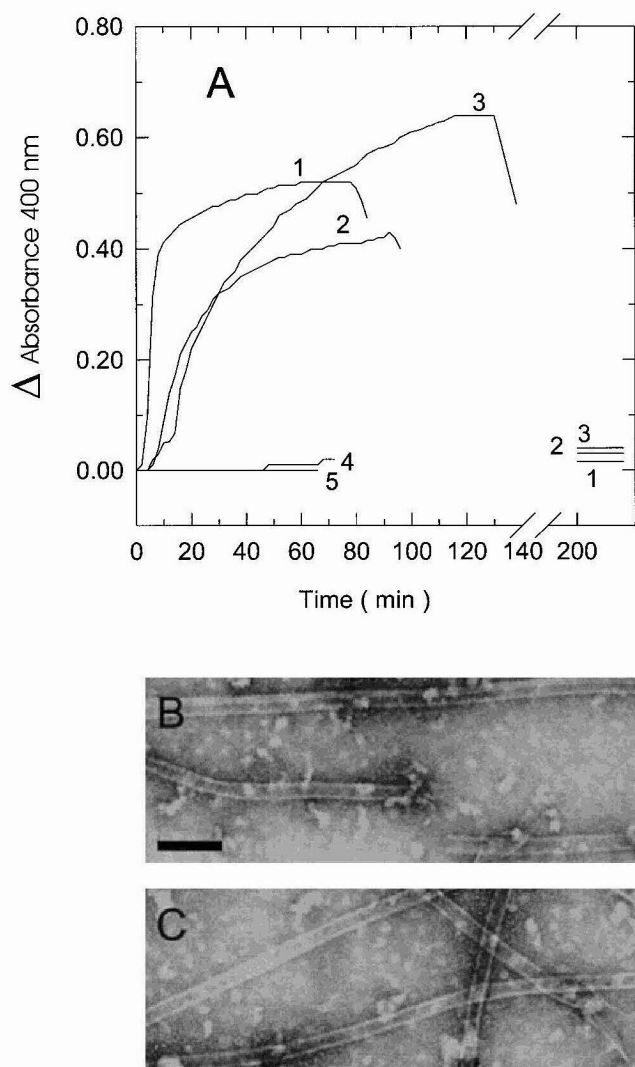
Fig. 2. Microtubule assembly induced by fluorescent taxoids. **A:** Turbidimetric records of 25 μM purified GDP-tubulin in PEGM buffer, pH 6.6 at 37°C, assembled with 30 μM taxol (1), FLUTAX (2), ROTAX (3), N-(4 -fluoresceincarbonyl)-L-alanine methyl ester (4) or 2 -Ac-FLUTAX (5). **B:** Electron micrograph of microtubules assembled with FLUTAX, negatively stained with uranyl acetate. **C:** Microtubules assembled with ROTAX. Bar = 100 nm.

lin at varying total FLUTAX concentrations indicated an apparent stoichiometry of one FLUTAX bound per tubulin (not shown).

Taxoid-induced assembly of GDP-tubulin is a rigorous equilibrium protein condensation polymerization, in which the critical protein concentration (the minimal concentration required for assembly) is, to a good approximation, equivalent to the apparent equilibrium constant of dissociation of one αβ-tubulin molecule from the microtubule end [Oosawa and Asakura, 1975; see Díaz et al., 1993]. The measurements of Figure 3A indicate critical concentrations of FLUTAX and ROTAX which

are, respectively, two- and fourfold larger than that of taxol. Comparative critical concentration measurements analyzed with the theory of linked functions [Wyman and Gill, 1990; Díaz et al., 1993] have indicated that the magnesium dependence of the FLUTAX-induced polymerization is more pronounced than that of taxol, with 2.9, instead of 1.9, additional Mg^{2+} ions bound per tubulin polymerized (Fig. 3B). The pH dependence is slightly less pronounced (0.2 instead of 0.5 additional H^+ ions per tubulin) and the effect of temperature is more pronounced for FLUTAX than for taxol (the value of the apparent van't Hoff enthalpy change was 123 instead of 64 kJ mol^{-1}) (not shown).

Spectrofluorometric measurements of ligand bound to the microtubule pellets confirmed that each assembled tubulin dimer binds 0.97 ± 0.08 FLUTAX molecules (not shown), the same as taxol [Díaz and Andreu, 1993]. FLUTAX was also bound by preassembled microtubules containing microtubule associated proteins in an approximately unitary ratio with the tubulin dimers, although FLUTAX precipitation in Pipes buffer prevented accurate quantitation (not shown). Measurements of competition between FLUTAX and taxol for binding to microtubules (Fig. 3C, points) are quantitatively described by a simple model of binding to the same microtubule site (solid lines), with an apparent dissociation constant 8 times larger for FLUTAX than for taxol.

Spectroscopic Changes in Fluorescent Taxoid upon Binding to Microtubules

The fluorescence spectrum and lifetime of the fluorescein chromophore covalently bound to 7-alanyl-taxol, as well as the chromophore ionization constant, are very similar to those of free fluorescein in solution. Although FLUTAX was initially designed as a taxol derivative substituted at nonessential position 7 [Kingston, 1994], very probably out of the binding site, it has turned out to be a microenvironment-sensitive probe. Interestingly, when FLUTAX is bound to microtubules, there is a 3-nm red shift in the absorption band of the fluorescein dianion (493 nm) and an increase relative to the absorption of the shoulder at 464 nm (Fig. 4A and Table I). These changes could be determined with accuracy by comparison with the inactive controls N-(4 -fluoresceincarbonyl)-L-alanine methyl ester and 2 -Ac-FLUTAX, showing that the fluorescein dianion, the emitting species in FLUTAX (Fig. 4B), is preferentially bound by microtubules. This suggests a cationic microenvironment around the fluorescent probe in microtubules. Comparative titrations have indicated a small but significant down shift of 0.3 ± 0.1 pH units in the apparent pK_a of FLUTAX upon binding to microtubules relative to its value in free solution (6.54 ± 0.03) (M.P. Lillo et al., unpublished observations).
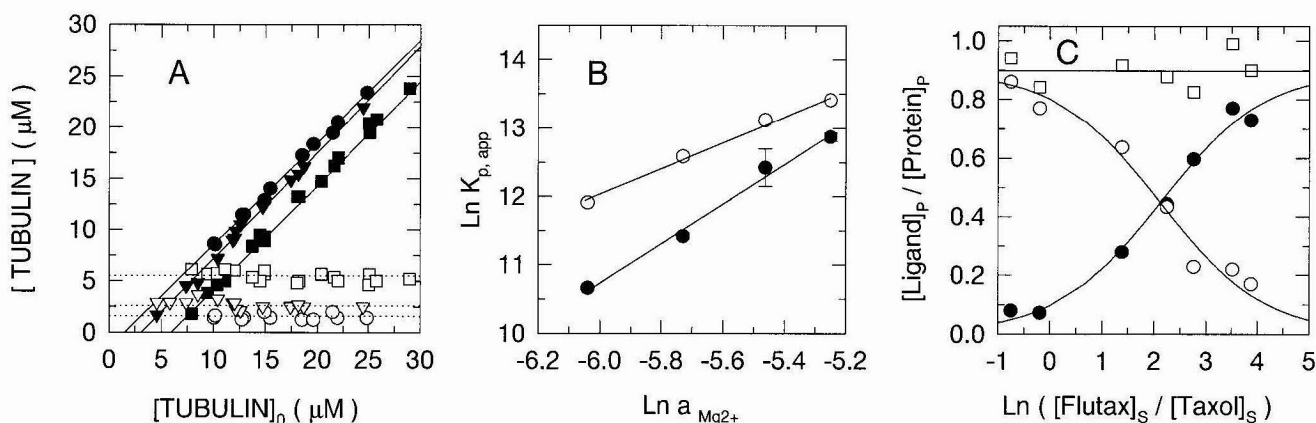
Fig. 3. **A:** Critical concentration (C_r) plots for GDP-tubulin assembly with taxol (**circles**, C_r 1.5 μM), FLUTAX (**triangles**, C_r 2.6 μM), and ROTAX (**squares**, C_r 5.5 μM), under same conditions as Figure 2. The concentration of pelleted protein (**filled symbols**) and protein in the supernatant (**open symbols**) is plotted as a function of total tubulin concentration. **B:** Linkage graphs [Wyman and Gill, 1990] of the apparent elongation constant $K_{p,app} = C_r^{-1}$ of FLUTAX (**filled circles**) and taxol-induced (**open circles**) polymerization of tubulin versus activity of Mg^{2+} ions. The slopes (2.9 and 1.9, respectively) are equal to the increment of Mg^{2+} ions preferentially bound by the tubulin polymer over the protomer. **C:** Competition of FLUTAX (**filled circles**) and taxol (**open circles**) for binding to microtubules assembled from 45 μM GDP-tubulin and 50 μM total taxoid. The experiment was performed essentially as described for docetaxel and taxol [Díaz and Andreu, 1993], in PEGM buffer at pH 7.0 and 37°C; 75–82% of total tubulin was assembled. The ratio of free FLUTAX to free taxol concentration (abscissa) was measured in the supernatant. It was modified by varying the ratio total FLUTAX/total taxol. The extents of binding of FLUTAX (**filled circles**) and taxol (**empty circles**) change, whereas their sum (**squares**) remains practically constant. The lines are the best fit to a simple model of competition for the same site in assembled tubulin [Díaz and Andreu, 1993], which indicates a ratio of apparent affinities of FLUTAX to taxol of 0.12.
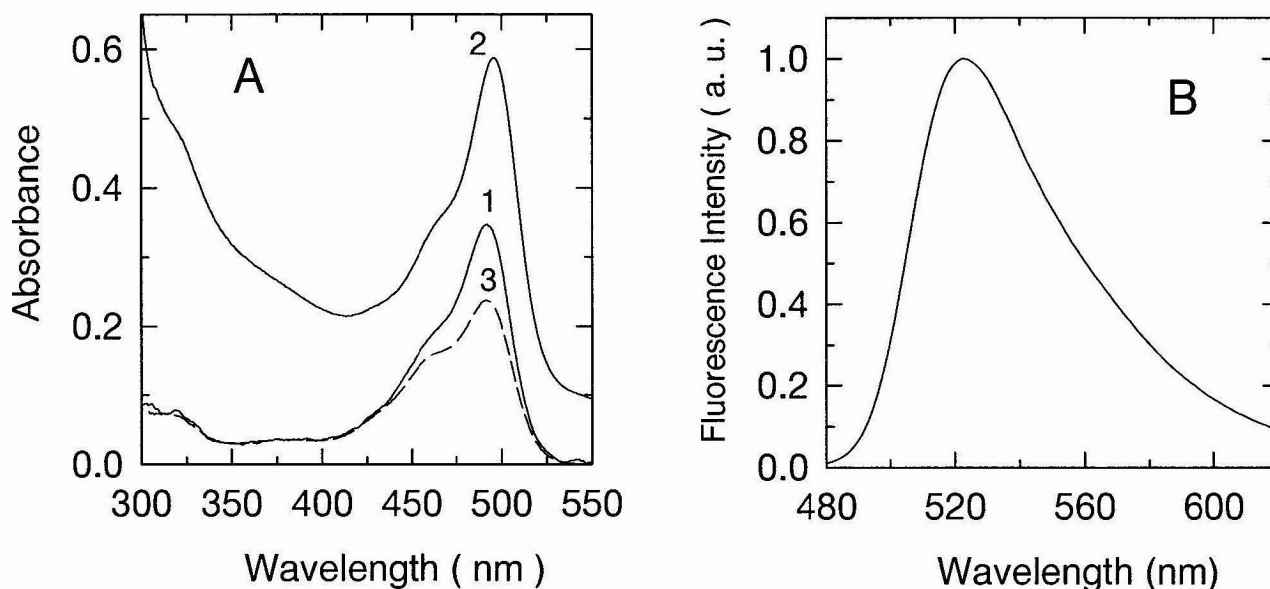

Fig. 4. **A:** Absorption spectra of free FLUTAX, 2 μM in PEGM buffer, pH 6.6 (**line 1**, absorbance multiplied by 10), FLUTAX bound to microtubules (20 μM, **line 2**; same conditions plus 25 μM tubulin, notice the light scattering due to microtubules) and free FLUTAX, 20 μM in the same buffer (**dashed line 3**, shown for comparison; notice the absorption changes due to FLUTAX aggregation). **B:** Corrected fluorescence spectrum of FLUTAX in microtubules ($\lambda_{ex} = 470$ nm, slit 2 nm). The normalized spectrum of free FLUTAX in buffer was marginally wider at the red side.

The stationary fluorescence anisotropy (r) of FLUTAX increased by an order of magnitude, to 0.2, when bound to microtubules, compared with the value in solution (Table I); nevertheless, this is still one-half of what would be observed for the completely immobilized dye $r_0(470) = 0.38$ [Chen and Bowman, 1965]. The fluorescence lifetime of FLUTAX in solution and bound to microtubules was the same (4.5 nsec). The time-

TABLE I. Spectroscopic Parameters of Free and Microtubule-Bound FLUTAX in PEMG Buffer at 37°C

FLUTAX	Concn (μM)	λ_{abs}^{max} (nm)	$\lambda_{em}^{max\ a}$ (nm)	$\epsilon_{496}^{apar\ b}$ ($M^{-1}\ cm^{-1}$) $\pm 3,000$	OD_{493}/OD_{464} ± 0.05	$Q_F^{rel\ c}$	τ (ns)^d ± 0.2	r^e ± 0.004	ϕ (ns)^f	r_∞^f
Free, PEGM (pH 6.6)	2	492	522	33,000	1.8	0.8	—	0.028	—	—
Free, PEGM (pH 7.0)	2	493	522	43,000	2.1	1.0	—	0.030	—	—
Bound, PEGM (pH 6.6)	20	496	522	46,000	2.1	0.8	4.5	0.20	4 ± 1	0.06

^{a}Corrected emission spectra. λ_{ex} = 470 nm, slit 2 nm.
^{b}Effective molar absorption coefficient.
^{c}Relative fluorescence yield: λ_{ex} = 470 nm, bandwidth 2 nm (reference Q_F = 1.0 for FLUTAX, 2 μM in PEGM buffer, pH 7.0).
^{d}Fluorescence decays were best fitted to a single exponential lifetime model.
^{e}Steady-state fluorescence anisotropy. λ_{ex} = 470 nm, λ_{em} = 520 nm, slit 2 nm.
^{f}Anisotropy relaxation time (ϕ), and residual anisotropy (r_∞). λ_{ex} = 380 nm, λ_{em} > 500 nm (cutoff filter).

resolved analysis of r(t) contains a very fast (hundreds of picoseconds) initial depolarization (from $r_0(380)$ = 0.24 to 0.18) that could not be resolved with our instrumentation. This is followed by a slower depolarization process, with a time constant of 4 ± 1 nsec, to finally attain a residual value r_∞ = 0.06 (Table I). The biphasic depolarization results from the very fast unrestricted angular motions of the dye moiety, followed by a slower motion with its supporting molecular structures, while the non-zero residual r_∞ value is characteristic of the angular restrictions imposed to probe rotation by the protein matrix. (Note that application of the diffusion-in-a-cone model [Kinosita et al., 1977] results in wobbling semi-angles of 66° and 80° for the fast and slow motions, respectively. A possible alternative to account for the time-dependent depolarization might be the resonant transfer of energy between identical chromophores (homo-transfer) [Van der Meer et al., 1994]. However, the contribution of homotransfer to the depolarization in the present case is considered to be less than 20%. This upper limit was obtained from the changes observed in anisotropy by FLUTAX excitation in the red edge of its absorption spectra [Valeur and Weber, 1978]. In addition, numerical modelling of the transfer rate in a microtubule lattice excludes homotransfer as a cause of the very fast initial depolarization).

Observation and Self-organization of Microtubules With Fluorescent Taxoids

Microtubules assembled from GDP-tubulin with FLUTAX and ROTAX are readily visualized under the fluorescence microscope, either as individual microtubules or with different degrees of entanglement (Fig. 5A,B). Radial structures resembling asters could be observed in microtubule samples assembled between glass slide and coverslip at room temperature (inset, Fig. 5B). Dense microtubule bundles (Fig. 5C) consistently formed, irrespective of microtubules being polymerized either in a tube at 37°C or directly between glasses. When microtubules were assembled from tubulin and MAPs, the further addition of FLUTAX resulted in rapid (<1

min) labeling with the fluorescent taxoid, as shown in Figure 5D. This confirmed that FLUTAX binds to microtubules irrespective of MAPs (see above) and suggested that the fluorescent taxoid would also bind to cellular microtubules.

Specific Labeling of Microtubules and Centrosomes of Cytoskeletons With FLUTAX: Comparison With Anti-tubulin Antibodies

FLUTAX (1 μM) was found to bind to, and stabilize, microtubules of unfixed PtK2 cytoskeletons in PBS, making microtubules readily observable under the fluorescence microscope (not shown). Fixation of cytoskeletons with formaldehyde or methanol destroyed the FLUTAX binding sites (fixation of cells incubated with 20 μM FLUTAX with 3.7% formaldehyde and methanol gave the same result). However, fixation with 0.2% glutaraldehyde permitted the simultaneous visualization of microtubules with both FLUTAX and monoclonal antibodies to tubulin. As shown in Figure 6A,B,C,D, the same individual cytoplasmic microtubules can be stained by FLUTAX and the DM1A antibody, although the taxoid detected somewhat weakly the fixed microtubules. Binding of FLUTAX is specific, since (1) it is displaced by excess docetaxel (50 μM, not shown), and (2) most of the microtubules disappear by previous cell treatment with the powerful inhibitor CI980(0.25 μM) [De Inés et al., 1994] (Fig. 6C,D). There are several important differences with respect to antibodies. FLUTAX stained centrosomes more accurately and brightly than the antibody, both in interphase (Fig. 6C,D) and in mitotic cells (Fig. 6E,J) and stained astral microtubules less intensely than the antibody. Two bright spots could be frequently resolved with FLUTAX in the centrosomes of interphase cells. The anaphase and telophase spindles frequently showed a characteristic dark line at the equator, corresponding to the midzone of the cleavage furrow, when cytoskeletons fixed with 0.2% glutaraldehyde were visualized by immunofluorescence with DM1A (Fig. 6H) and other antibodies to tubulin (not shown; note that this zone may be stained after methanol fixation). However, micro-
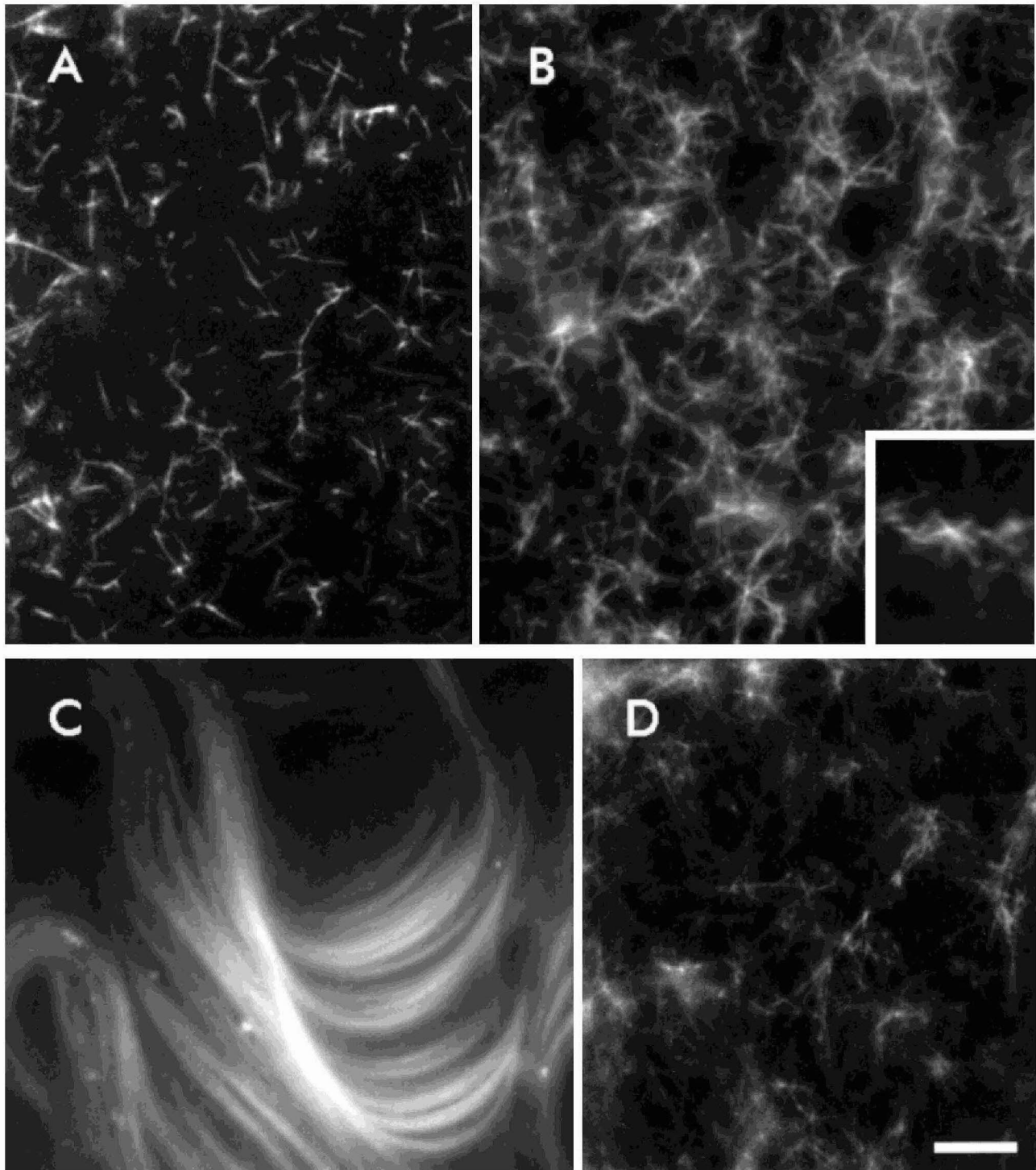
Fig. 5. Microtubules imaged with fluorescent taxoids under the epifluorescence microscope **A:** Microtubules assembled with 25 μM tubulin and FLUTAX. **B:** Another view of FLUTAX microtubules; **inset:** a radial aster-like formation of FLUTAX microtubules. **C:** Bundles of ROTAX microtubules. **D:** Microtubules assembled with MAPs and visualized immediately after addition of FLUTAX and dilution to 0.4 mg ml^{-1} microtubule protein. Bar = 10 μm.
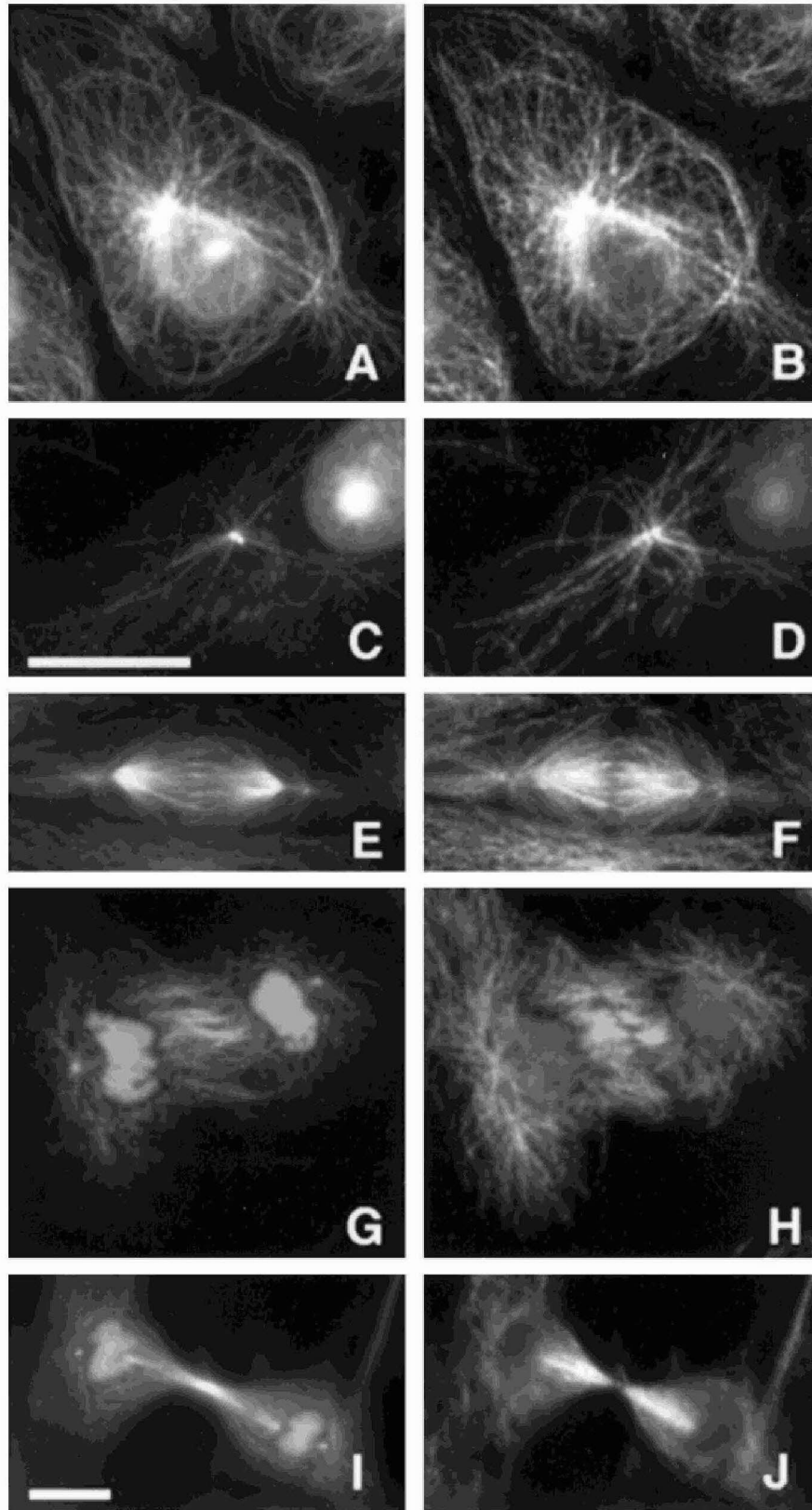
Fig. 6. Simultaneous binding of FLUTAX (**A,C,E,G,I**) and the DM1A monoclonal antibody to tubulin (indirect immunofluorescence (**B,D,F,H,J**) to mildly fixed PtK2 cytoskeletons. A,B: Interphase cells. C,D: Cells treated with 0.25 μM CI980 for 4 hr to depolymeryze microtubules. E,F: Anaphase spindle. G,H: Telophase spindle. I,J: Cytokinesis. Bars = 10 μm. Bar in C for C and D; bar in I for all other panels.

tubules were clearly labeled in the midzone by FLUTAX (Fig. 6E,G). Consequently, the central zone of midbodies was much more strongly stained by the taxoid (Fig. 6I). It should be noted that marked staining of the central zone of midbodies was also observed with ROTAX in unfixed cytoskeletons (not shown) and with FLUTAX in living cells (see Fig. 9).

To further characterize the centrosomal staining with FLUTAX, it was compared to detection with TU-30 monoclonal antibody to γ-tubulin [Nováková et al., 1996], after recording the corresponding FLUTAX images of cytoskeletons. The two bright spots labeled by FLUTAX in interphase cells, presumably corresponding to two centrioles (Fig. 7A), coincide with the zone detected by the antibody to γ-tubulin (Fig. 7B). Co-localization was equally observed after centrosomal division in prophase (Fig. 7E,F) and in anaphase cells (Fig. 7I,J), and only one FLUTAX spot per centrosome was distinguished in these cases.

Observation of Unfixed Cellular Microtubules and Living Cells With FLUTAX

Optimal microtubule visualization was obtained shortly after (<1-min) FLUTAX addition to unfixed Ptk2 cytoskeletons in PEM microtubule-stabilizing buffer. ROTAX gave microtubular images, but also nonmicrotubular vesicular staining, possibly due to the binding of rhodamine to other organelles, and its use with cells was not further pursued. FLUTAX is a specific microtubule visualization probe, since the microtubule images were reduced to the centrosomes and a few microtubules of Ptk2 cells by pretreatment with 10 μM colchicine (not shown) and were erased by an excess of nonfluorescent taxoid in a few minutes, or with 2′-Ac-FLUTAX instead of FLUTAX (Fig. 8A,B; note that the nucleolar staining by FLUTAX in cytoskeletons is nonspecific, since it is not displaced by an excess of nonfluorescent taxoid). On the other hand, treatment of a variety of cells with 1 μM FLUTAX during 0.5–4 hr, or culturing the cells with subinhibitory concentrations of the probe, followed simply by removal of excess medium and directly mounting the coverslips with 70% glycerol-containing buffer, gave good images of the cellular microtubule network, typically with less background than immunofluorescence of fixed cells. Representative examples of Ptk2 epithelial cells, U937 leukemia cells, neuro2A neuroblastoma cells, and *Trypanosoma cruzi* directly stained with FLUTAX are presented in Figure 8C–F, respectively. Each of these images disappeared when 50 μM docetaxel was added to the cultures simultaneously with FLUTAX (not shown).

The images shown in Figure 8C–F do not result from FLUTAX internalized and bound by living cells, but its intensity is mainly due to entry of residual FLUTAX by rupture of the plasma membrane during mounting, and

fast binding to microtubules. In fact, observation of intact Ptk2 cells with 1–30 μM FLUTAX in culture medium gave much weaker images. However, incubation of growing U937 human leukemia cells with 15 nM FLUTAX during 16 hr permitted visualization of centrosomes and attached fibrillar structures in interphase cells (Fig. 9A,B), prophase spindle poles (Fig. 9C,D), the two half-spindles in metaphase (Fig. 9E,F), anaphase (Fig. 9G,H), and the mid-body in cytokinesis (Fig. 9I,J). Again, all images were ligand-specific, since localized fluorescence was completely abolished when 1 μM docetaxel was added to the cell cultures 4 h before observation (Fig. 9K,L). This low FLUTAX concentration had an insignificant effect on the cell cycle of U937 cells (Fig. 9M,N).

DISCUSSION
Fluorescent Taxoids as Microtubule Probes

FLUTAX constitutes a specific probe for the taxol binding site of microtubules, which induces the assembly of purified tubulin into microtubules with similar overall properties and slightly lower efficiency than the parent drug taxol. FLUTAX binds to one site per assembled dimer, competing with taxol with eightfold weaker apparent affinity. The enhanced Mg^{2+} dependency of FLUTAX-induced microtubule elongation (compared to taxol) indicates the presence of one additional Mg^{2+} ion bound per tubulin polymerized. This cation is not necessarily localized, although it might be in complex with the anionic fluorescein chromophore, which undergoes a red shift, indicating a decreased polarity and/or ion pair formation. Interestingly, the change detected in the fluorescein absorption spectrum upon FLUTAX binding to microtubules is evidence of a cationic microenvironment of the fluorescein group attached to position 7 of taxol, compatible with the proximity of a metal cation or of some basic residues of tubulin, even the protein as a whole has a net negative charge. In this context, fluorescent N(dimethylamino)benzoyl taxol derivatives at positions 7 and 10 have been reported to probe a less hydrophobic environment in microtubules than 2- and N-(derivatives) [Sengupta et al., 1997].

Analysis of the time-resolved fluorescence data indicates that FLUTAX binds to microtubules in a way that allows considerable freedom of motion of the bulky fluorescein group, with little steric restrictions from the protein. The simplest interpretation is that the taxoid is bound on a microtubule surface (or into a cleft commensurate with the tubulin monomer), with the C-7 and C-10 side of the taxane ring system pointing to the solvent. This observation may help to locate the taxol binding site in microtubules. It is compatible with the easy accessibility of the taxoid binding site in in vitro assembled microtubules [Dye et al., 1993; Díaz and Andreu, unpub-
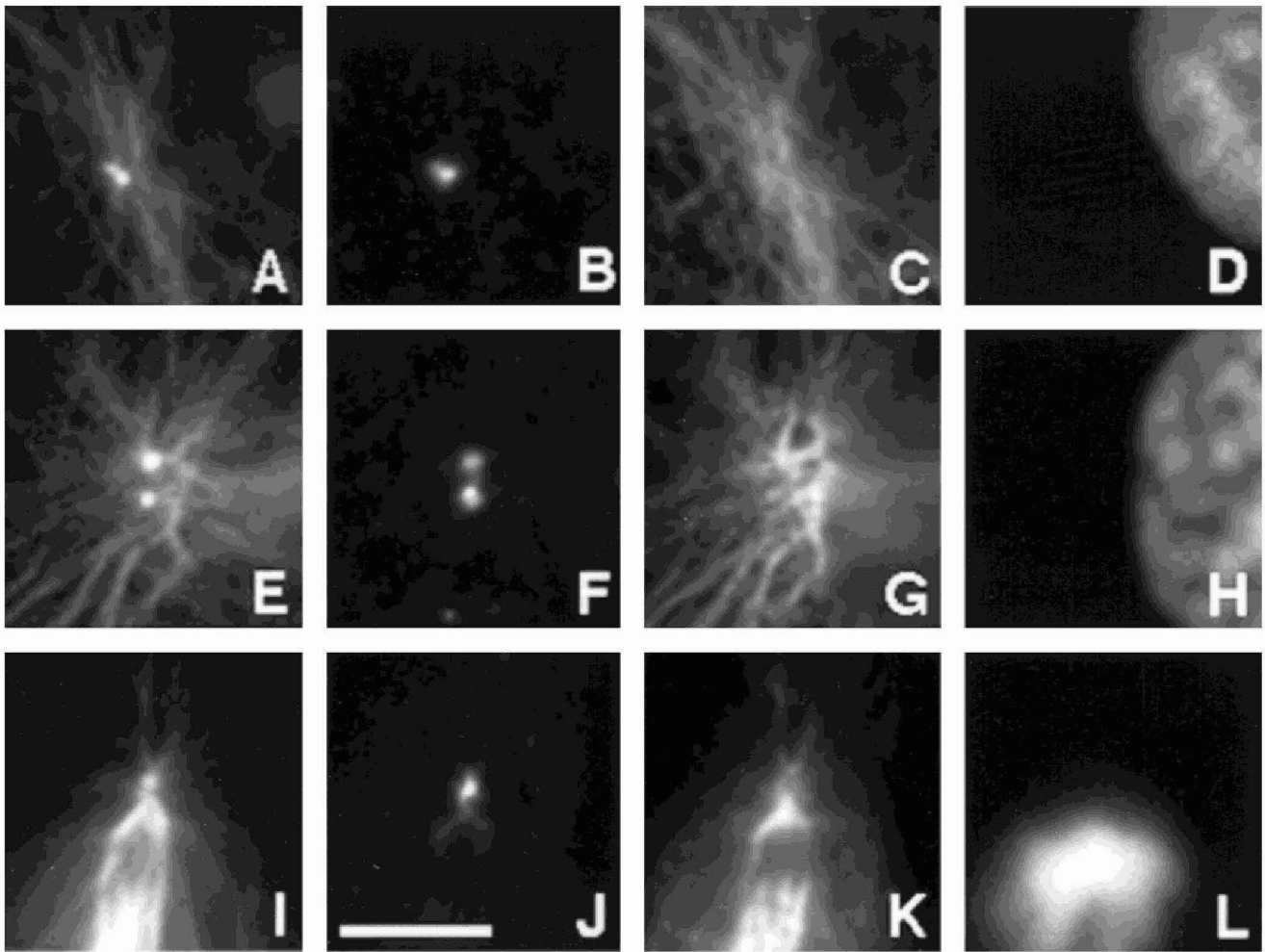
Fig. 7. Comparison of the centrosomal area visualized with FLUTAX and TU-30 monoclonal antibody to γ-tubulin. PtK2 cytoskeletons were labeled with FLUTAX (**A,E,I**), then fixed and simultaneously stained with monoclonal antibody to γ-tubulin (**B,F,J**), α-tubulin (**C,G,K**), and Hoescht 33342 (**D,H,L**). Cell A–D was in interphase, cell E–H in prophase, and cell I–L in anaphase. Bar = 5 μm.

lished observations; this study] and in cellular microtubules (this study), and with the report of an anti-idiotypic antibody that mimics taxol [Leu et al., 1994]. It is in apparent contrast with the high-resolution model structure of tubulin in taxol-stabilized zinc-sheets, in which taxol is at one side of the β-tubulin monomer in the face corresponding to the microtubule lumen [Nogales et al., 1997]. If taxol would bind to microtubules in the same locus as in the zinc sheets, our results would require an orientation of C-7 facing the microtubule lumen, which would be a potentially functional compartment. If, on the contrary, the taxol site is at the outer microtubule wall, position C-7 should be at the outer microtubule surface. FLUTAX rapidly (<1 min) labels preassembled MAP-containing microtubules. It is difficult to explain how taxol and FLUTAX could get into the microtubule lumen, but through the open microtubule ends or by microtubule

dynamic instability (unless there is an unexpectedly large channel or breathing of the protein structure permitting FLUTAX to get through the microtubule wall). However, MAPs suppress in vitro dynamic instability [Horio and Hotani, 1986]. Simplified calculations of diffusion-limited binding indicate that FLUTAX could diffuse into microtubules and label them from the end along 10 μm in a minimum time of 4 min with 10 μM free ligand in the bulk solution (40 min with 1 μM ligand), due to the high density of binding sites that have to be filled in the microtubule (see Appendix). This is difficult to conciliate with the above observation and argues against a location of the taxol binding site at the microtubule lumen.

A similar chemical strategy to FLUTAX might in principle be employed to prepare gold cluster taxol derivatives and locate the taxol binding sites in microtubules and in cells with electron cryo-microscopy. It is also
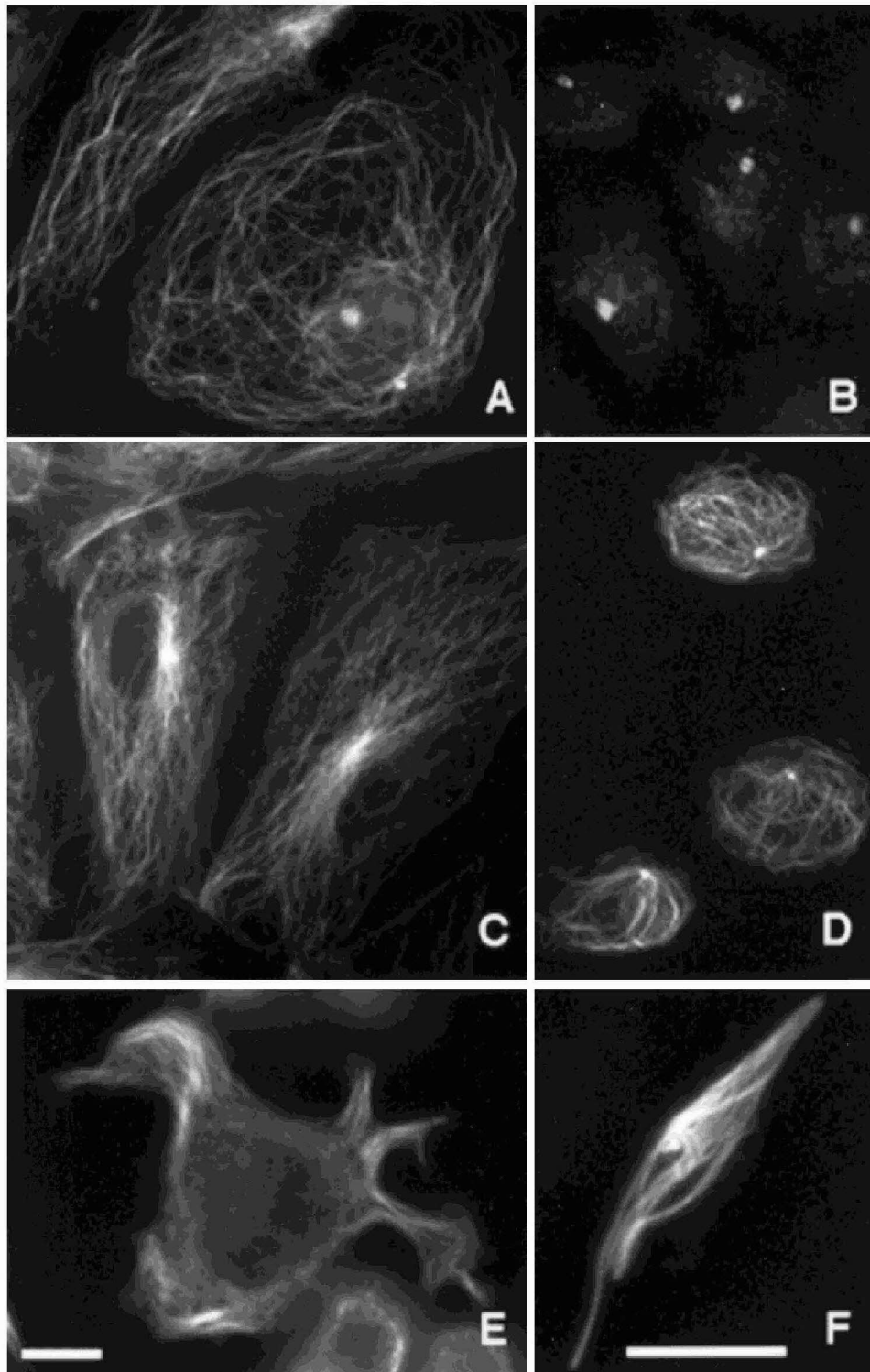
Fig. 8. Specific visualization of cellular microtubules with FLUTAX. A: PtK2 cytoskeletons (Fig. 5) were not fixed, but were incubated with 1 μM FLUTAX for 1 hr. Similar images were obtained at approximately 1 min after the addition of FLUTAX (not shown). B: Same as A, but with the addition of 50 μM docetaxel; Incubation with 2-Ac-FLUTAX gave a similar image (not shown). C: PtK2 cells incubated with 0.5 μM FLUTAX for 20 hr and directly mounted. D: U937 cells incubated with 37 nM FLUTAX for 16 hr. E: Neuro2A cells incubated with 1 μM FLUTAX for 2 hr. F: Trypanosoma cruzi epimastigotes incubated with 1 μM FLUTAX for 3 hr. Note that images (C–F) correspond to permeabilized cells, since (1) only the cells whose chromatin was stained with propidium iodide had microtubules strongly stained by FLUTAX; (2) cells treated with FLUTAX for very short times also developed staining; (3) cells mounted without glycerol had much weaker FLUTAX microtubule patterns, although a few were similarly stained; and (4) cells mounted without glycerol, but whose plasma membrane had been solubilized with 0.025% (v/v) Nonidet P-40, had microtubule images similar to those in A. Bars in E (for A–E) and in F = 10 μm.
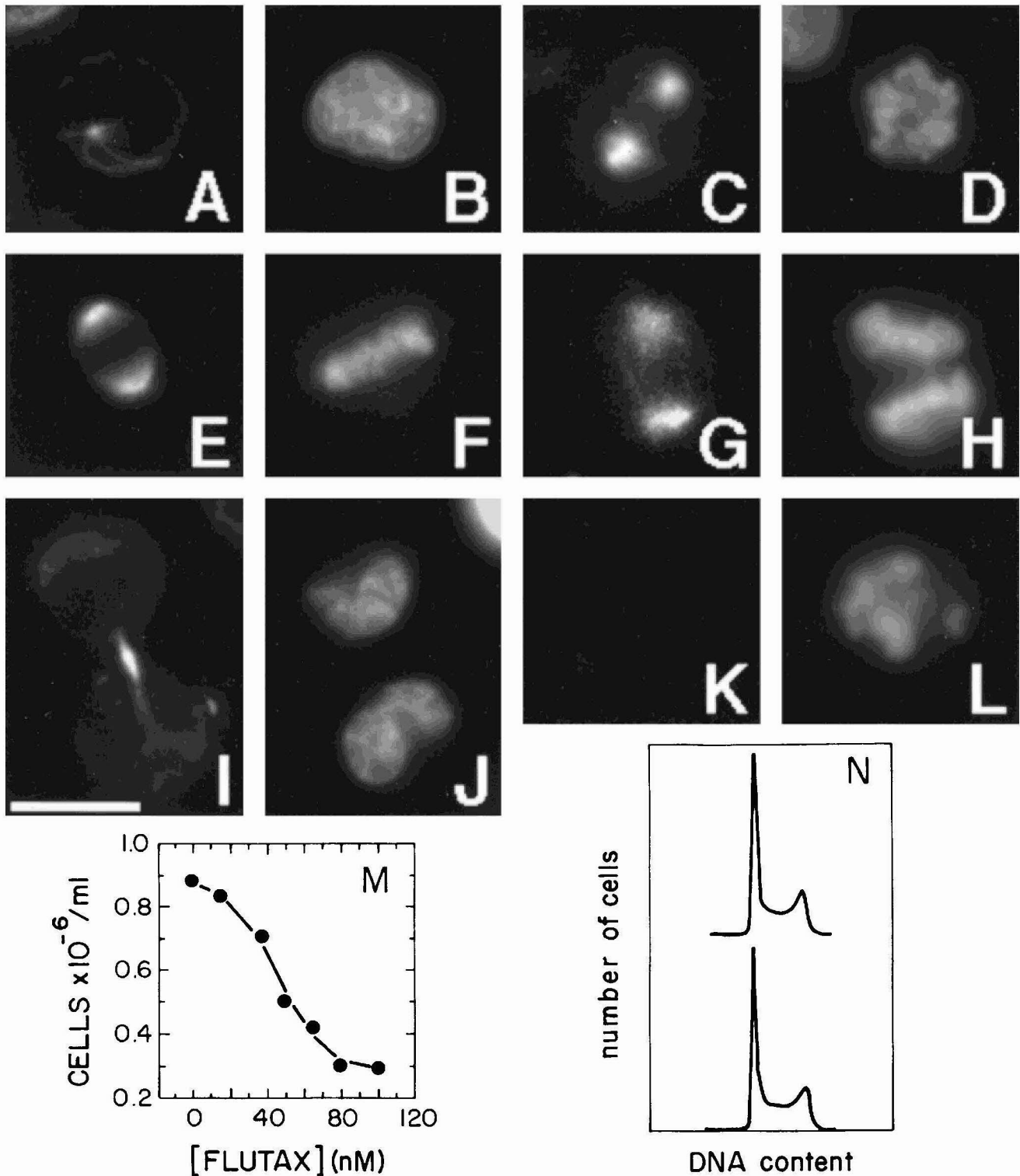
Fig. 9. Microtubules visualized with FLUTAX in live cells. U937 cells were cultured 16 hr with 15 nM FLUTAX and imaged with FLUTAX (**A,C,E,G,I,K**) and Hoescht 33342 (**B,D,F,H,J,L**). Cell K–L was additionally incubated with 700 nM docetaxel for the last 4 hr. Cell A–B illustrates interphase, cell C–D prophase, cell E–F metaphase, cell G–H anaphase and cell I–J cytokinesis. **M:** Inhibition of cell growth as a function of FLUTAX concentration. 200,000 cells per ml were cultured with different concentrations of FLUTAX during 24 hr. Live cells excluding Trypan blue were counted with a hemocytometer. **N:** Identical cytofluorometric profiles of untreated U937 cells (top profile) and cells cultured with 15 nm FLUTAX (bottom profile). The flow cytometric analysis was performed as described [De Inés et al., 1994]. Bar = 10 μm.

appealing to try and probe the taxol binding sites in living cells with the spectroscopic methods outlined in this study. Other possible applications of FLUTAX and the rhodamine derivative ROTAX include the detection of nuclei of taxoid-induced microtubule assembly with fluorescence spectroscopy and analytical ultracentrifugation, and the study of the molecular recognition kinetic mechanisms of ligand binding and dissociation to the taxol binding site of microtubules. FLUTAX and ROTAX may be employed in fluorescence energy transfer experiments (R_0 5.5 nm) with microtubules. However, it should be noted that multiple FLUTAX molecules bind nonspecifically to dimeric tubulin, giving absorption changes opposite to those due to its binding to microtubules, fluorescence lifetime heterogeneity, and a smaller steady-state fluorescence anisotropy (unpublished observations).

Microtubules induced by FLUTAX and ROTAX are readily observed with fluorescence microscopy. Taxol and taxoid-stabilized microtubules are frequently employed for a variety of experimental purposes, including preparation of microtubule proteins from diverse sources [Collins and Vallee, 1987] and studies of motor proteins [Gilbert et al., 1995; Kikkawa et al., 1995; Sosa and Milligan, 1996], for which direct visualization of microtubules with the fluorescent taxoids might be useful, provided that the fluorescent group would not interfere with the properties investigated. On the other hand, the taxoid-induced microtubules in a crowded solution of elongated polymers [Hitt et al., 1990; Mandelkow et al., 1989; Tabony, 1994] undergo spontaneous organization into dense bundles (Fig. 5), possibly related to cellular microtubule bundles. This simple level of self-organization of tubulin and taxoid proceeds without the microtubule motors and DNA required for the in vitro assembly of asters and bipolar spindles [Heald et al., 1996]. Radial structures also observed in the tubulin–taxoid solutions resemble asters induced by taxol in cells [De Brabander et al., 1981; Verde et al., 1991], although we cannot rule out that they result from microtubule adhesion to dust particles or to aggregated tubulin.

Green Fluorescent Taxoids Specifically Label Polymerized Cellular Tubulin

The direct labeling of native cellular binding sites with the fluorescent taxoid FLUTAX gives new insights into the microtubule cytoskeleton and opens new possibilities for its study. It has been hypothesized that taxol may actually be a surrogate of endogenous cellular microtubule inducers or stabilizers [Schiff et al., 1979; Suffness, 1994]. The observations that FLUTAX homogeneously labels microtubules of Ptk2 cytoskeletons in less than 1 min after its addition into the microtubule-stabilizing buffer (supposedly no elongation) and also labels stable

flagellar microtubules, suggest that the taxol binding site is at the outer (see above), instead of the inner microtubule surfac [Nogales et al., 1997]. This may imply that either taxol would bind to different loci in microtubules and zinc sheets, or that the face to which it binds in the sheets does not correspond to the inner microtubule wall. On the other hand, low doses of the fluorescent taxoid on cultured cells might bind to the more actively growing microtubules while inhibiting their dynamics.

In addition, we have found that the fluorescent taxoid binds not only to microtubules, but stains centrosomes more brightly than commonly used antibodies to tubulin. This may be attributable to a more facile access to the microtubular structures forming the centrioles [Tournier and Bornens, 1994] or to a hypothetical enhanced reactivity with certain tubulin isotypes. An important question is whether γ-tubulin in ring complexes in the pericentriolar material [Zheng et al., 1995; Moritz et al., 1995] and in other locations [Moudjou et al., 1996] might also bind taxol, or if this is an exclusive property of β-tubulin polymerized into microtubules. The results shown in Figure 7 suggest that the two spots observed with FLUTAX in interphase cells correspond to the separated or duplicating centrioles. The single-spot centrosomal labeling in lysed mitotic cells may result from the optically unresolved staining of the two centrioles in the centriole pair. These results suggest that centrosomes, in addition to microtubules may be targets of taxol action. The strong FLUTAX labeling at the centrosomal region may also be due to active nucleation of tubulin polymerization. This is supported by the strong polar labeling of spindles in live mitotic cells (Fig. 9). The observation that FLUTAX labels spindle microtubules at the cell equatorial plane where antibodies can give a dark zone suggests that microtubules are there precluded from reaction with antibodies by other structures, such as the telophase plate [Andreassen et al., 1991]. Another explanation is enhanced binding to actively growing free microtubule plus ends, compared to the kinetochore-attached ends and to minus ends at the poles [Inoué and Salmon, 1995]. The stronger labeling by FLUTAX of centrosomes, spindle poles, spindle equators, and midbodies over cytoplasmic microtubules, taken together, suggests that the fluoresceinated taxol is predominantly labeling cellular sites where tubulin is more actively polymerized. A recent study of the sites of binding of rhodamine-tubulin in lysed cells presents images [Méda et al., 1997] closely resembling those obtained with FLUTAX in this study.

The direct observation of microtubules with FLUTAX in permeabilized cells (cytoskeletons, or in many cases cells simply mounted with glycerol) presents an advantage over indirect immunofluorescence and does not require microinjection of individual cells to introduce the probe. It allows diverse morphological applications,

including for example the taxonomy and cell cycle characterization of flagellates and ciliates. Qualitative comparison of microtubule visualization in PtK2 cells and cytoskeletons have indicated that the FLUTAX derivative with fluorine atoms in positions 2 and 7 of its fluorescein moiety, and the same difluoro-FLUTAX but with a sulfonic acid group instead of the 2 -carboxylic group, behave comparably to FLUTAX. Both analogues have improved photostability and are highly soluble and biochemically active, even slightly less potent mitotic inhibitors than FLUTAX (Souto et al., unpublished observations). In our comparison, FLUTAX (Souto et al., 1995) stains microtubules somewhat better than the compound with a longer spacer 7-O-[N-(4 -fluorescein-carboxamido-n-hexanoyl)-L -alanyl]taxol (unpublished observations), but much better than ROTAX, 7-O-[N-(4 - sulforhodaminesulfonyl)-β-alanyl]taxol, a compound based on the same chemical strategy [Guy et al., 1996], 7-O-[N-(4 -sulforhodaminesulfonyl)-L-alanyl]taxol (unpublished) and 3 -BODYPY-FL-Taxol (Molecular Probes P-7500) (not shown). For a comparison with the weakly active nitrobenzoxadiazol derivatives of docetaxel at positions 7 and 3 , see Dubois et al. [1995]. A very weak visualization of some spindles was obtained with CU-TAX [Souto et al., 1995] employing near-UV fluorescence microscope optics, which was not observed with the biochemical probe 2-debenzoyl-2-(m-aminobenzoyl)taxol [Han et al., 1996]; microtubule visualization with (dimethylamino)benzoyl taxoid probes [Sengupta et al., 1997] has not been documented. Therefore, whereas we have obtained several active green fluorescent taxoids and have employed them for the first time to label cellular microtubules specifically, efficiently and accurately, comparable red and blue fluorescent taxoids are not yet available.

One potential apparently paradoxical application of the fluorescent taxoids is the visualization of microtubules in growing cells. This requires that a concentration window exists in which the taxoid does not appreciably inhibit cell division (possibly the microtubule dependent process which is most taxoid-sensitive), but marginally binds to microtubules, thus permitting their visualization based on the high sensitivity of the fluorescence probe and adequate detection methods. This has only been realized in favorable cases at a limited resolution (Fig. 9). Finally, FLUTAX can also be used to visualize the targets of taxoid binding in living tumor cells treated with cell cycle inhibitory concentrations. This has very recently been accomplished with U937 and K562 human leukemia cells; the results (to be reported elsewhere) include primary labeling of centrosomes and spindles and the induction and visualization of multiple asters and microtubule bundles.

In conclusion, the fluoresceinated taxoid FLUTAX, one of a series of active taxol derivatives, interacts specifically with the taxol binding site, probably at the outer microtubule surface, making them both directly and rapidly observable under the fluorescence microscope. If, on the contrary, the taxoid binding site were at the lumen, this would confer unforeseen functionality to the inner microtubule surface in interactions with relatively small molecules. FLUTAX detects centrosomes, mitotic spindle poles, and midbodies, more strongly than with immunofluorescence. Low probe concentrations permit for the first time the direct imaging of centrosomes and of microtubules during mitosis in growing human leukemia cell cultures.

REFERENCES

Andreassen, P.R., Palmer, D.K., Wener, M.H., and Margolis, R.L. (1991): Telophase disc: A new mammalian mitotic organelle that bisects telophase cells with a possible function in cytokinesis. J. Cell. Sci. 99:523–534.

Andreu, J.M., and Timasheff, S.N. (1984): The measurement of cooperative protein self-assembly by turbidity and other techniques. Methods Enzymol. 130:47–59.

Andreu, J.M., Bordas, J., Diaz, F., Garcia de Ancos, J., Gil, R., Medrano, F.J., Nogales, E., Pantos, E., and Towns-Andrews, E. (1992): Low resolution structure of microtubules in solution. Synchroton X-ray scattering and electron microscopy of taxol-induced microtubules assembled from purified tubulin in comparison with glycerol- and Map-induced microtubules. J. Mol. Biol. 226:169–184.

Andreu, J.M., Diaz, J.F., Gil, R., De Pereda, J.M., Garcia de Lacoba, M., Peyrot, V., Briand, C., Towns-Andrews, E., and Bordas, J. (1994): Solution structure of taxotere-induced microtubules to 3 nm resolution. The change in protofilament number is linked to the binding of the taxol side chain. J. Biol. Chem. 269:31785–31792.

Arévalo, M.A., Nieto, J.M., Andreu, D., and Andreu, J.M. (1990): Tubulin assembly probed with antibodies to synthetic peptides. J. Mol. Biol. 214:105–120.

Arnal, I., and Wade, R.H. (1995): How does taxol stabilize microtubules? Curr. Biol. 5:900–908.

Atkins, P.W. (1978): "Physical Chemistry." San Francisco: W.H. Freeman.

Baum, S.G., Wittner, M., Nadler, J.P., Horwitz, S.B., Dennis, J.E., Schiff, P.B., and Tanoowitz, H.B. (1981): Taxol, a microtubule stabilizing agent, blocks the replication of Trypanosoma cruzi. Proc. Natl. Acad. Sci. U.S.A. 78:4571–4575.

Carlier, M.F., and Pantaloni, D. (1983): Taxol effect on tubulin polymerization and associated guanosine-5 -triphosphate hydrolysis. Biochemistry 22:4814–4822.

Cassimeeris, L.U., Pryer, N.K., and Salmon, E.D. (1988): Real-time observations of microtubule dynamic instability in living cells. J. Cell Biol. 107:2223–2231.

Chen, R.F., and Bowman, R.L. (1965): Fluorescence polarization: measurement with ultraviolet-polarizing filters in a spectrofluorometer. Science 147:729–732.

Clark, J.I., and Garland, D. (1978): Fluorescein colchicine. Synthesis, purification and biological activity. J. Cell Biol. 76:619–627.

Collins, C.A., and Vallee, R.B. (1987): Temperature-dependent reversible assembly of taxol-treated microtubules. J. Cell. Biol. 105:2847–2854.

De Brabander, M., Geuens, G., Nuydens, R., Willebrords, R., and De Mey, J. (1981): Taxol induces the assembly of free microtubules in living cells and blocks the organizing capacity of the centrosomes and kinetochores. Proc. Natl. Acad. Sci. U.S.A. 78:5608–5612.

De Inés, C., Leynadier, D., Barasoain, I., Peyrot, V., Garcia, P., Briand, C., Rener, G.A., and Temple, C. Jr. (1994): Inhibition of microtubules and cell cycle arrest by a new 1-deaza-7,8-dihydropteridine antitumor drug, CI 980, and by its chiral isomer, NSC 613863. Cancer Res. 54:75–84.

De Pereda, J.M., Wallin, M., Billger, M., and Andreu, J.M. (1995): Comparative study of the colchicine binding site and the assembly of fish and mammalian microtubule proteins. Cell Motil. Cytoskeleton 30:153–163.

Derry, W.B., Wilson, L., and Jordan, M.A. (1995): Substoichiometric binding of taxol suppresses microtubule dynamics. Biochemistry 34:2203–2211.

Diaz, F., and Andreu, J.M. (1993): Assembly of purified GDP-tubulin into microtubules induced by taxol and taxotere: Reversibility, ligand stoichiometry and competition. Biochemistry 32:2747–2755.

Díaz, J.F., Menendez, M., and Andreu, J.M. (1993): Thermodynamics of ligand-induced microtubule assembly. Biochemistry 32:10067–10077.

Díaz, J.F., Andreu, J.M., Diakun, G., Towns-Andrews, E., and Bordas, J. (1996): Structural intermediates in the assembly of taxoid-induced microtubules and GDP-tubulin double rings: Time-resolved X-ray scattering. Biophys. J. 70:2408–2420.

Dubois, J., Le Goff, M.T., Gueritte-Voegelein, F., Guenard, D., Tollon, Y., and Wright, M. (1995): Fluorescent and biotinylated analogues of docetaxel: Synthesis and biological evaluation. Biorg. Med. Chem. 3:1357–1368.

Dye, R.B., Fink, S.P., and Williams, R.C. (1993): Taxol-induced flexibility of microtubules and its reversal by Map-2 and Tau. J. Biol. Chem. 268:6847–6850.

Gilbert, S.P., Webb, M.R., Brune, M., and Johnson, K.A. (1995): Pathway of processive ATP hydrolysis by kinesin. Nature 373:671–676.

Guy, R.K., Scott, Z.A., Sloboda, R.D., and Nicolaou, K.C. (1996): Fluorescent taxoids. Chem. Biol. 3:1021–1031.

Han, Y., Chaudhary, A.G., Chordia, M.D., Sackett, D.L., Perez-Ramirez, B., Kingston, D.G.I., and Bane, S. (1996): Interaction of a fluorescent derivative of paclitaxel (Taxol) with microtubules and tubulin-colchicine. Biochemistry 35:14173–14183.

Heald, R., Tournebize, R., Blank, T., Sandaltzopoulos, R., Becker, P., Hyman, A., and Karsenti, E. (1996): Self-organization of microtubules into bipolar spindles around artificial chromosomes in Xenopus egg extracts. Nature 382:420–425.

Hitt, A.L., Cross, A.R., and Williams, R.C., Jr. (1990): Microtubule solutions display nematic liquid crystalline structure. J. Biol. Chem. 265:1639–1647.

Horio, T., and Hotani, H. (1986): Visualization of the dynamic instability of individual microtubules by dark-field microscopy. Nature 321:605–607.

Horwitz, S.B. (1992): Mechanism of action of taxol. Trends Pharm. Sci. 13:134–136.

Inoué, S., and Salmon, E.D. (1995): Force generation by microtubule assembly/disassembly in mitosis and related movements. Mol. Biol. Cell 6:1619–1640.

Kikkawa, M., Ishikawa, T., Wakabayashi, T., and Hirokawa, N. (1995): Three-dimensional structure of the kinesin head–microtubule complex. Nature 376:274–277.

Kingston, D.G. (1994): Taxol: The chemistry and structure–activity relationships of a novel anticancer agent. Trends Biotech. 12:117–125.

Kinosita, K., Jr. Kawato, S., and Ikegami, A. (1977): A theory of fluorescence polarization decay in membranes. Biophys. J. 20:389–305.

Lee, J.C., and Timasheff, S.N. (1975): The reconstitution of microtubules from purified calf brain tubulin. Biochemistry 14:5183–5187.

Leu, J.G., Chen, B.X., Diamandouros, A.W., and Erlanger, B.F. (1994): Idiotypic mimicry and the assembly of a supramolecular structure: an anti-idiotypic antibody that mimics taxol in its tubulin-microtubule interactions. Proc. Natl. Acad. Sci. U.S.A. 91:10690–10694.

Mandelkow, E., Mandelkow, E.M., Hotani, H., Hess, B., and Müller, S.C. (1989): Spatial patterns from oscillating microtubules. Science 246:1291–1293.

Manfredi, J.J., Parness, J., and Horwitz, S.B. (1982): Taxol binds to cellular microtubules. J. Cell Biol. 94:688–696.

Mateo, C.R., Lillo, M.P., Gonzalez-Rodriguez, J., and Acuña, A.U. (1991): Molecular order and fluidity of plasma membrane of human platelet from time-resolved fluorescence depolarization. Eur. Biophys. J. 20:41–52.

Méda, P., Chevrier, V., Eddé, B., and Job, D. (1997): Demonstration and analysis of tubulin binding sites on centrosomes. Biochemistry 36:2550–2558.

Mellado, W., Magri, F.N., Kingston, D.G.I., Garcia-Arenas, R., Orr, G.A., and Horwitz, S.B. (1984): Preparation and biological activity of taxol acetates. Biochem. Biophys. Res. Commun. 124:329–336.

Mickey, B., and Howard, J. (1995): Rigidity of microtubules is increased by stabilizing agents. J. Cell Biol. 130:909–917.

Moll, E., Manz, E., Mocikat, S., and Zimmermann, H.P. (1982): Fluorescent deacetylcolchicine. Exp. Cell. Res. 141:211–220.

Moritz, M., Braunfeld, M.B., Sedat, J.W., Alberts, B., and Agard, D.A. (1995): Microtubule nucleation by γ-tubulin-containing rings in the centrosome. Nature 378:638–640.

Moudjou, M., Bordes, N., Paintrand, M., and Bornens, M. (1996): γ-Tubulin in mammalian cells: the centrosomal and cytosolic forms. J. Cell Sci. 109:875–887.

Nicolaou, K.C., and Guy, R.K. (1995): The conquest of taxol. Angew. Chem. Int. Ed. Engl. 34:2079–2090.

Nogales, E., Wolf, S.G., Khan, I.A., Ludueña, R.F., and Downing, K.H.

(1995): Structure of tubulin at 6.5 Å and location of the taxol-binding site. Nature 375:424–427.

Nogales, E., Wolff, S.G., and Downing, K.H. (1997): Structure of the tubulin dimer. Presented at the EMBO Syposium Structural Biology, Heidelberg, pp. 6–7. Nature, (in press).

Nováková, M., Dráverová, E., Schürman, W., Czihak, G., Viklický, V., and Draber, P. (1996): γ-Tubulin redistribution in taxol-treated mitotic cells probed by monoclonal antibodies. Cell Motil. Cytoskeleton 33:38–51.

Oosawa, F., and Asakura, S. (1975): "Thermodynamics of the Polymerization of Protein." London: Academic Press.

Panda, D., Daijo, J.E., Jordan, M.A., and Wilson, L. (1995): Kinetic stabilization of microtubule dynamics at steady state in vitro by sub-stoichiometric concentrations of tubulin-colchicine complex. Biochemistry 34:9921–9929.

Parness, J., and Horwitz, S.B. (1981): Taxol binds to polymerized tubulin in vitro. J. Cell Biol. 91:479–487.

Rao, S., Krauss, N.E., Heerding, J.M., Swindell, C.S., Ringel, I., Orr, G.A., and Horwitz, S.B. (1994): 3 -(p-Azidobenzamido)taxol photolabels the N-terminal 31 aminoacid of β-tubulin. J. Biol. Chem. 269:3132–3134.

Rao, S., Orr, G.A., Chaudhary, A.G., Kingston, D.G.I., and Horwitz, S.B. (1995): Characterization of the taxol binding site on the microtubule: 2-(m-Azidobenzoyl)taxol photolabels a peptide (amino acids 217-231) of β-tubulin. J. Biol. Chem. 270:20235–20238.

Schiff, P.B., and Horwitz, S.B. (1980): Taxol stabilizes microtubules in mouse fibroblast cells. Proc. Natl. Acad. Sci. U.S.A. 77:1561–1565.

Schiff, P.B., Fant, J., and Horwitz, S.B. (1979): Promotion of microtubule assembly in vitro by taxol. Nature 277:665–667.

Schuck, P. (1996): Kinetics of ligand binding to receptor immobilized in a polymer matrix. Biophys. J. 70:1230–1249.

Schulze, E., and Kirschner, M. (1986): Microtubule dynamics in interphase cells. J. Cell Biol. 104:277–288.

Sengupta, S., Boge, T.C., Liu, Y., Hepperle, M., Georg, G.I., and Himes, R.H. (1997): Probing the environment of tubulin-bound paclitaxel using fluorescent paclitaxel analogues. Biochemistry 36:5179–5184.

Song, D., Hsu, L.H., and Ay, L.S. (1996): Binding of taxol to plastic and glass containers and protein under in vitro conditions. J. Pharm. Sci. 85:29–31.

Sosa, H., and Milligan, R.A. (1996): Three-dimensional structure of ncd-decorated microtubules obtained by a back-projection method. J. Mol. Biol. 260:743–755.

Souto, A.A., Acuña, A.U., Andreu, J.M., Barasoain, I., Abal, M., and Amat-Guerri, F. (1995): New fluorescent water-soluble taxol derivatives. Angew. Chem. Int. Ed. Engl. 34:2710–2712.

Suffness, M. (1994): Is taxol a surrogate for a universal regulator of mitosis? In Vivo 8:867–878.

Tabony, J. (1994): Morphological bifurcations involving reaction-diffusion processes during microtubule formation. Science 264:245–248.

Tagliaferro, W.H., and Pizzi, T. (1955): Connective tissue reactions in normal and immunized mice to a reticulotropic strain of Trypanosoma cruzi. J. Infect. Dis. 96:199–226.

Taylor, E.W. (1965): The mechanism of colchicine inhibition of mitosis. J. Cell. Biol. 25:145–160.

Tournier, F., and Bornens, M. (1994): Cell cycle regulation of centrosome function. In Hyams, J.S., and Lloyd, C.W. (eds.): "Microtubules." New York: Wiley-Liss, pp 303–324.

Vale, R.D., Coppin, C.M., Malik, F., Kull, F.J., and Milligan, R.A. (1994): Tubulin GTP hydrolysis influences the structure, mechanical properties and kinesin-driven transport of microtubules. J. Biol. Chem. 269:23769–23775.

Valeur, B., and Weber, G. (1978): A new red-edge effect in aromatic molecules: Anomaly or aparent rotation revealed by fluorescence polarization. J. Chem. Phys. 69:2393–2400.

Van der Meer, B.W., Cooker, G. III, and Chen, S.Y.S. (1994): "Resonance Energy Transfer." VCH Publishers, p 20.

Venier, P., Maggs, A.C., Carlier, M.F., and Pantaloni, D. (1994): Analysis of microtubule rigidity using hydrodynamic flow and thermal fluctuations. J. Biol. Chem. 269:13353–13360.

Verde, F., Berrez, J.M., Antony, C., and Karsenti, E. (1991): Taxol-induced microtubule asters in mitotic extracts of Xenopus eggs: Requirement of phosphorylated factors and cytoplasmic dynein. J. Cell Biol. 112:1177–1187.

Weisenberg, R.C. (1972): Microtubule formation in vitro in solutions containing low calcium concentration. Science 177:1104–1105.

Weisenberg, R.C., Borisy, G.G., and Taylor, E.W. (1968): The colchicine binding protein of mammalian brain and its relation to microtubules. Biochemistry 7:4466–4479.

Williams, H.J., Moyna, G., Scott, A.I., Swindell, C.S., Chirlian, L.E., Heerding, J.M., and Williams, D.K. (1996): NMR and molecular modeling study of the conformation of taxol 2 -acetate in chloroform and aqueous dimethyl sulfoxide solutions. J. Med. Chem. 39:1555–1559.

Wilson, L., and Friedkin, M. (1966): The biochemical events of mitosis. Biochemistry 5:2462–2468.

Wilson, L., and Jordan, M.A. (1994): Pharmacological probes of microtubule function. In Hyams, J.S., and Lloy, C.W. (eds.): "Microtubules." New York: Wiley-Liss, pp 59–84.

Wolff, S.G., Nogales, E., Kikkawa, M., Gratzinger, D., Hirokawa, N., and Downing, K.H. (1996): Interpreting a medium-resolution model of tubulin: comparison of zinc-sheet and microtubule structure. J. Mol. Biol. 262:485–501.

Wolfson, M., Yang, C.P.H., and Horwitz, S.B. (1997): Taxol induces tyrosine phosphorylation of Shc and its association with Grb-2 in murine RAW 264.7 cells. Int. J. Cancer 70:248–252.

Wulf, F.A., Debonen, F.A., Bautz, Faulstich, H., and Wieland, Th. (1979): Fluorescent phallotoxin, a tool for the visualization of cellular actin. Proc. Natl. Acad. Sci. U.S.A. 76:4498–4502.

Wyman, J., and Gill, S. (1990): "Binding and Linkage. Functional Chemistry of Biological Macromolecules." Mill Valley, CA: University Science Books.

Zheng, Y., Wong, M.L., Alberts, B., and Mitchison, T. (1995): Nucleation of microtubule assembly by a γ-tubulin-containing ring complex. Nature 378:578–583.

APPENDIX

The minimum time required to label the inner wall of microtubules with FLUTAX can be estimated by assuming that the fast, practically irreversible, binding to the wall is limited only by diffusion of the ligand [see appendix in Schuck, 1996] into the tube. As ligand molecules enter the tube, they bind to vacant sites, from the ends to the center. By setting the number of molecules bound by the tube layer of thickness dx equal to the number of molecules that diffuse into the tube during the time interval dt, assuming a linear spatial gradient of free FLUTAX, and applying Fick's first law, one obtains an expression for dt as a function of x, the distance from the tube end to the binding front (the leading edge of the growing zone of saturated FLUTAX binding sites). Integrating this expression with respect to x leads to the

following expression for the time required for the binding front to move from the end of the tube to position x:

$$t(x) = [B]_0/[A](x^2/2D) \qquad (1)$$

where $[B]_0$ is the effective total concentration of binding sites within the tube, $[A]$ the ligand concentration in the bulk solution and D the diffusion coefficient in the tube, assumed to be the same as in the solution. Note that if D or $[A]$ is lower than in the bulk solution [Schuck, 1996] the time $t(x)$ will be longer. Similarly, if binding is slower than diffusion, $t(x)$ will increase. For molecules of the size of FLUTAX, the effective hydrodynamic radius and the diffusion coefficient are in the range of 1 nm and 2×10^{-6} cm^2 s^{-1}, respectively. The local concentration of binding sites (tubulin dimers) per microtubule lumen volume is in the order of 10 mM, estimated from the microtubule lattice and dimensions (13 dimers per turn, 8-nm axial displacement, approximately 15-nm inner diameter). The bulk probe concentration is ~1 μM in our experiments with permeabilized cells, and in the range of 10 μM for microtubules assembled with tubulin and MAPs. This gives estimated minimum times to fill a microtubule along 10 μm with FLUTAX of ~40 and ~4 min, respectively. For comparison, microtubule turnover in interphase cells proceeds end-wise and requires about 15 min [Schulze and Kirschner, 1986]. Typical rates of cellular microtubule rapid shortening and elongation are 17 and 7 μm min^{-1}, respectively, an average cycle of shortening and elongation extending for 6–8 μm and lasting 1.5 min [Cassimeeris et al., 1988]. Simple diffusion without binding into the tube follows the expression:

$$t(x) = x^2/2D \qquad (2)$$

[Atkins, 1978] would take place in the sub-second time scale; however, this would not optically label the tube, since the inner probe concentration is the same as in the background solution. Microtubules could become visible with substoichiometric FLUTAX binding, however, 10 μM ligand will essentially saturate the microtubule binding sites (one FLUTAX per tubulin dimer, not shown).